JOURNAL OF CATALYSIS **158,** 288–300 (1996)
ARTICLE NO. 0028

Non-ASF Product Distributions Due to Secondary Reactions during Fischer–Tropsch Synthesis

E. W. Kuipers,[1] C. Scheper, J. H. Wilson, I. H. Vinkenburg, and H. Oosterbeek

Koninklijke/Shell Laboratorium Amsterdam, P.O. Box 38000, 1030 BN Amsterdam, The Netherlands

Received May 3, 1995; revised September 5, 1995; accepted September 6, 1995

Since Fischer–Tropsch (FT) synthesis is a chain growth reaction, its total product yield decreases exponentially with chain length forming a so-called Anderson–Schulz–Flory (ASF) distribution. Such a distribution is unselective toward middle distillates for all possible chain growth probabilities. Chain-length-dependent secondary reactions, however, cause deviations from the ASF-type distribution and can thus be used to improve the selectivity to the desired product range. To investigate secondary reactions we set out to study FT synthesis on flat model catalysts, a cobalt foil and cobalt particles on a SiO_2 wafer, allowing a much better definition of the experiments than porous ones. On a Co foil olefin hydrogenation is the main chain-length-dependent secondary reaction, causing an exponential increase in the paraffin-to-olefin ratio with carbon number, but not resulting in a deviation from the ASF distribution. On Co/SiO_2 model catalysts chain-length-dependent reinsertion of α-olefins into the chain growth process is the main secondary reaction, causing an increase of the growth probability with chain length. To a lesser extent, hydrogenolysis also plays a role, shortening long hydrocarbons by successive demethylation. On Co/SiO_2 the interplay of chain-length-dependent reinsertion and hydrogenolysis results in sigmoid product distributions with a high selectivity to middle distillates. These product distributions can be fitted with a simple model in which a chain growth reaction is combined with chain-length-dependent secondary hydrogenation, reinsertion, and hydrogenolysis. © 1996 Academic Press, Inc.

INTRODUCTION

In the Fischer–Tropsch (FT) synthesis a mixture of CO and H_2, i.e., synthesis gas, is converted to hydrocarbons and H_2O over a heterogeneous catalyst containing a group VIII metal. To this end CO and H_2 are dissociated at the surface of the catalyst and at first converted into CH_x species and H_2O (1). Alkyl chains can subsequently be formed out of these initial species via a chain growth mechanism. These alkyl chains are chemically bound to the surface at the terminal carbon. Either a new $-CH_2-$ group can be inserted into this bond, or the bond to the surface can be broken, thus terminating the chain growth. Principally two termination reactions are possible, namely α-hydrogenation, yielding a paraffin, or β-dehydrogenation, producing an α-olefin. Such a chain growth mechanism will yield a molar distribution decreasing exponentially with chain length, n, the so-called Anderson–Schulz–Flory (ASF) distribution. The exponential decrease reflects the chain growth probability, α, which is

$$\alpha = 1 - T^{\mathrm{par}} - T^{\mathrm{ol}}, \qquad [1]$$

where T^{par} and T^{ol} are the probabilities that a growing alkyl chain is terminated as a paraffin or an α-olefin, respectively. However, most FT product distributions reported in the literature strongly deviate from an ASF distribution. Practically all these deviations are caused by secondary reactions of the primary hydrocarbon product, such as reinsertion into the chain growth process, hydrogenation, and hydrogenolysis. It has previously been shown that the rates of reinsertion (2) and hydrogenation (3) increase exponentially with chain length. This exponential increase is caused by an enrichment of the longer hydrocarbons at the catalyst surface due to an n-dependent physisorption (3, 4) and solubility (3). To a much lesser extent diffusion limitations can also play a role (2, 3).

Thirty years ago Pichler *et al.* concluded that the primary α-olefin product is hydrogenated in a secondary reaction since they observed an increase of the paraffin-to-olefin ratio with an increase in catalyst contact time (5). This observation was later confirmed by many others (2–4, 6–8). A more direct measurement of the rate of secondary hydrogenation can be obtained by cofeeding olefins. Practically all cofeed studies show a considerable amount of secondary hydrogenation of the cofed olefins (3, 4, 8–27). Secondary hydrogenation is strongly inhibited by CO (3, 8, 10, 11, 28) and H_2O (8, 28).

Primary α-olefin product can also be reinserted into the chain growth process. Olefin reinsertion was first observed experimentally half a century ago by cofeeding studies (29,

[1] Present address: Shell Research Limited, Thornton Research Centre, P.O. Box 1, Chester CH1 3SH, England.

0021-9517/96 $12.00

30) and has since been confirmed many times (8–12, 18–22, 25, 27, 31–50). However, the impact of α-olefin reinsertion on the total product distribution became clear only a few years ago, mainly due to the work of Iglesia *et al.* (2, 8, 28). Reinsertion of an α-olefin into the chain growth process reverses the termination by β-dehydrogenation, causing an increase in the net chain growth probability (51). Since the reinsertion rate increases exponentially with chain length, the net chain growth probability increases from $(1 - T^{par} - T^{ol})$ to $(1 - T^{par})$ with increasing chain length, causing the commonly observed ''double ASF'' distribution (2, 8, 28). Thus reinsertion of olefins strongly influences the C_5^+ selectivity. According to Iglesia *et al.* a high coverage of CO favors the selective reattachment of olefins to chain growth sites (28), whereas the size of crystallites has no noticeable effect (52).

The group VIII metals which can catalyze the FT synthesis (Fe, Co, Ru), can also hydrogenolyze hydrocarbons in an H_2 atmosphere (53). On Fe and Co hydrogenolysis occurs by a successive demethylation (54), whereas on Ru the C–C bond breaking is less selective (55). The hydrogenolysis rate will drop sharply with CO pressure, because CO poisons C–C, C–H, and H–H bond breaking reactions. However, several studies have shown that under FT synthesis conditions a considerable amount of the produced olefins is still hydrogenolyzed (12, 18, 21, 23, 32, 40, 44, 46, 48, 56). The ''above ASF'' yield of CH_4 can be partly attributed to hydrogenolyis (18, 32, 44, 46, 57). Hydrogenolysis reverses the chain growth and can thus cause a drop in C_{10}^+ selectivity (51, 58–60). In the literature hardly any information can be found on the hydrogenolysis of paraffins during FT synthesis, although there are some indications that it can occur (18, 32, 61).

The primary hydrocarbon product can also undergo isomerization but we will not deal with this reaction in the present study.

Secondary reactions strongly influence the product spectrum of FT synthesis and can be used to optimise the selectivity to the desired product range. To this end we have investigated the impact of hydrogenation, reinsertion, and hydrogenolysis on the product spectrum. For this purpose we have used flat model catalysts, i.e., Co foils and Co particles on flat SiO_2 wafers. These flat catalysts offer several advantages. Cobalt can be easily prepared in various dispersions on flat supports using spin-coating (62, 63). Deposited on these flat supports the particles are directly accessible to analysis, e.g., the particle size distribution can be analysed using atomic force microscopy (AFM). But in this study of secondary reactions the most important advantage of flat model catalysts lies in their ability to permit testing under conditions of differential reaction. Since all particles are directly accessible from the gas phase no transport limitations, causing concentration gradients, have to be taken into account, suggesting a more straightforward interpretation of kinetic data. The behavior of the FT reaction can be measured in the complete absence of diffusion limitations.

This paper reports on catalytic tests of flat model catalysts, which yield product distributions that strongly deviate from an ASF distribution. These deviations will be explained using a model in which reinsertion of α-olefins into the chain growth mechanism and hydrogenolysis of paraffins are taken into account.

EXPERIMENTAL

The glass reactor used for the catalytic experiments has been described in a previous publication (3) Continuous ideally stirred tank reactor (CISTR) behavior is helped by a minor temperature gradient over the reactor causing additional ''stirring'' due to convection. The temperature of the sample is measured by a Chromel/Alumel thermocouple. The reactor is operated in flow mode at 1 bar total pressure. The total reactor volume is 10 cm^3. Both a quadrupole mass spectrometer (QMS) and a gas chromatograph (GC) (Chrompack 9001) are used to analyse the composition of the gas leaving the reactor on-line. The GC separation of C_1 to C_5 is done on a Poraplot Q column and C_6 to C_{22} are separated on a CP-Sil-5 column. Flame ionization detectors (FID) are used because of their high detection efficiency and linear response. CO, CO_2, O_2, H_2O, and H_2 are monitored by the QMS. To prevent condensation of products and to reduce the retention time during transport from the reactor to the GC, the tubes downstream are heated. It has been thoroughly checked that the results are not affected by condensation and retention. To this end it has at first been assured that the dew point concentrations at room temperature of the products are at least an order of magnitude larger than the concentrations produced. Next it has been assured that cofeeding much higher concentrations of the long hydrocarbons does not result in condensation in the setup. Retention times could also be obtained from cofeed experiments and for the longest hydrocarbons these did not exceed an hour. The test experiments were run for much longer times, the product distributions were measured every half hour, and it was made sure that they were not transient. Synthesis gas is prepared by mixing H_2 and CO via mass flow controllers, enabling any H_2/CO ratio to be obtained. Hexene can be added to the feed by using a gas mixture of 465 ppm in H_2. Other hydrocarbons can be added to the feed in the vapour phase by passing the syngas through a temperature controlled bubbler. Under standard reaction conditions (1 bar, 5 STP ml/min, 493 K, $H_2/CO = 2$) the activity of the empty reactor was too low to be detected. In the empty reactor no secondary reactions of cofed hydrocarbons were observed either.

As catalysts a poly-crystalline cobalt foil (Goodfellow,

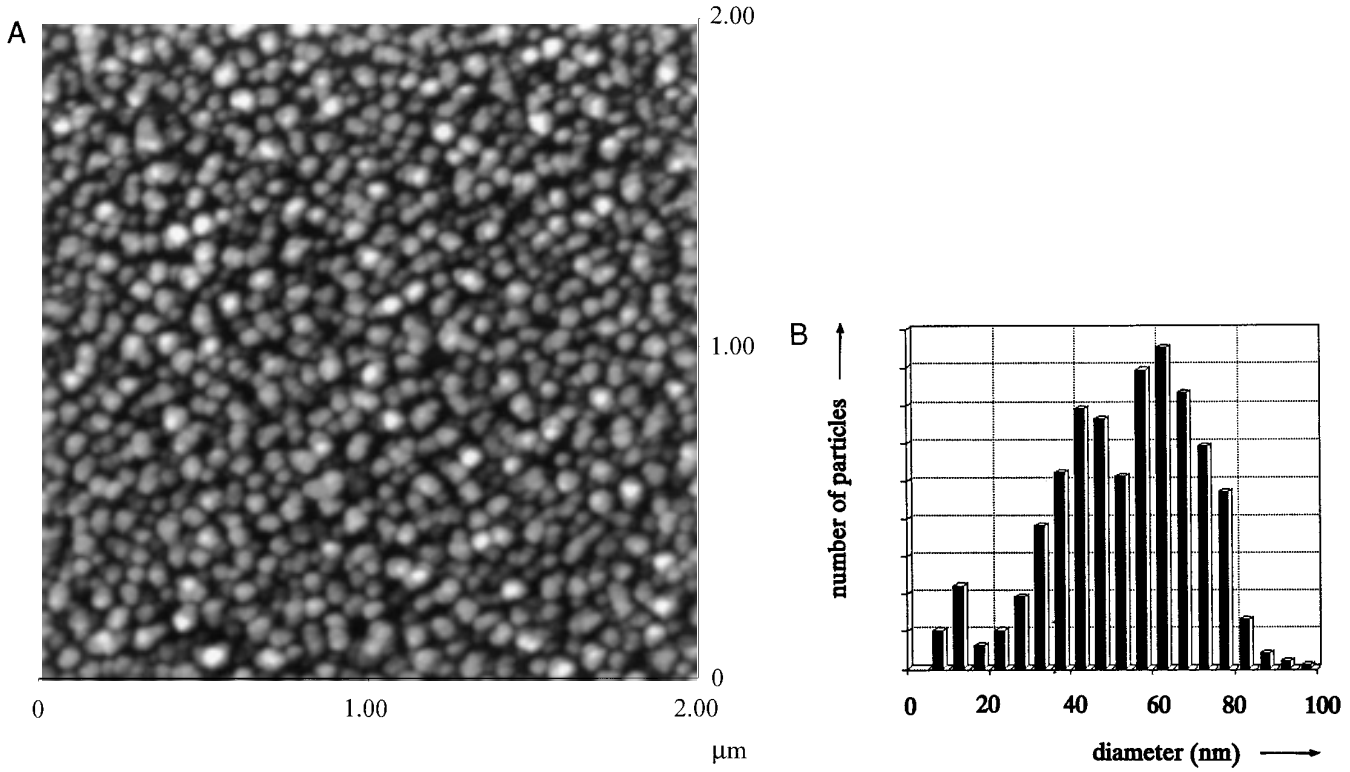

FIG. 1. (A) Atomic force microscopy image of cobalt particles obtained by spin-coating a solution of an anhydrous cobalt precursor in 1-butanol with a subsequent calcination in air. (B) Diameter distribution obtained by image analysis of Fig. 1a.

purity 99.99%, thickness 0.25 mm) and Co particles deposited on flat SiO_2 wafers were used. Prior to every experiment the Co foils were calcined in air at 673–723 K for 3 h. The Co foils were subsequently reduced in a H_2 flow (10 STP ml/min) at 1 bar and 573 K for 5 min. During the reduction the production of H_2O was monitored by the QMS. After reduction the H_2 flow was replaced by a flow of synthesis gas and reaction was carried out at 493 K. The flat SiO_2 wafers were prepared by calcination of polished single-crystalline 2-in. Si wafers (Si(100)) in air at 1273 K for 6 h resulting in a SiO_2 coating of around 70 nm as indicated by its Newton interference color. A high coverage of sub-micrometer Co particles was obtained by spin-coating a solution of an anhydrous cobalt precursor in 1-butanol (62, 63).

The Co precursor was subsequently calcined in air (60 K/h to 393 K, 2 h, 120 K/h to 673 K, 4 h). Prior to each experiment the catalyst was again calcined at 1073 K for 5 h. Calcination at such a high temperature caused considerable sintering of the oxidic cobalt phase in the first few hours, but hardly any additional sintering was observed during subsequent calcination treatments. The resulting sample has been analyzed by AFM. The micrograph is shown in Fig. 1a. The corresponding particle size distribution, as obtained by image analysis of the micrograph, is shown in Fig. 1b. In the nanometer range the AFM does not show the real particle size but a convolution of the AFM tip, which has a finite tip size (radius ± 5 nm), with the particle instead. Thus the particle size as given by the AFM is expected to be several nanometers larger than the real value (64). Both AFM and X-ray photoelectron spectroscopy (XPS) show that around half of the wafer is covered by cobalt oxide particles. The cobalt oxide particles are reduced in the reactor under a 1 bar H_2 flow at 573 K for 5 min. After reduction the H_2 flow is replaced by a flow of synthesis gas and reaction is carried out at 493 K. During all experiments conversions were extremely low, the concentration of the CH_4 produced being around 1500 ppm. Since the conversions are this low the carbon material balance is almost fully made up (>99%) by the unconverted CO. Thus if carbon builds up in the reactor/tubes, e.g., by the settling of long hydrocarbons, this would go unnoticed by making up the carbon material balance since it would result in a discrepancy much smaller than the best possible error bars with which the in- and outgoing CO flows can be determined. Thus the preciously discussed checks on impact of product condensation and retention are more appropriate criteria for these low conversion experiments.

For the case of a Co foil, standard reaction conditions

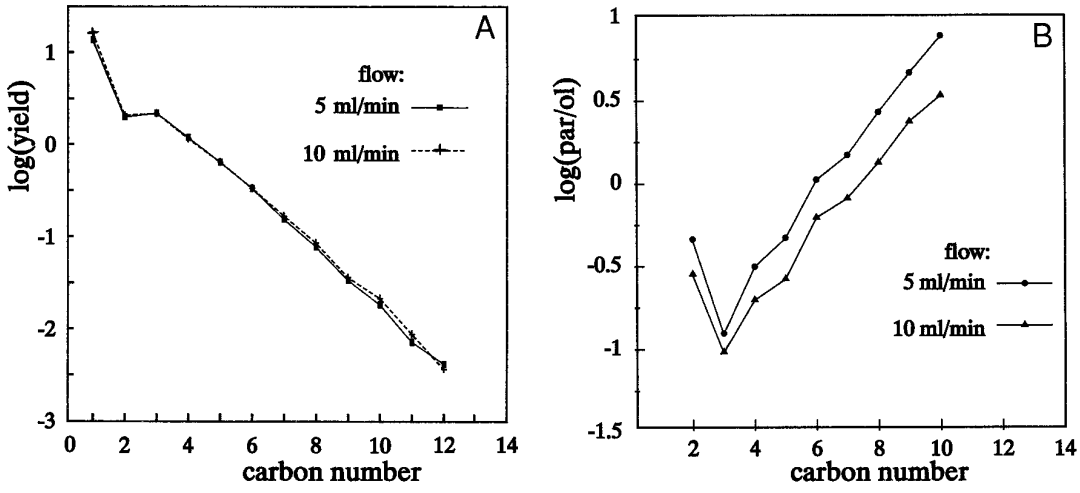

FIG. 2. (A) Total product yield (pmol/cm^2 · s) as a function of carbon number obtained for a 25-cm^2 Co foil (reduced at 573 K for 5 min) for two different flows, T = 493 K, H_2/CO = 2, P = 1 bar. (B) The corresponding paraffin-to-olefin ratios as a function of carbon number.

gave a specific activity for the turnover of CO of around 3×10^{14}/cm^2 · s, and a chain growth probability of 0.5, both comparable to values previously reported for polycrystalline Co and a stepped Co-single crystal surface (65, 66). The sub-micrometer particles of cobalt deposited on SiO_2 yielded comparable CO turn-over-numbers per cm^2 of cobalt surface area. The chain growth probability for the Co particles in the C_3–C_{10} range is around 0.7, which is larger than that obtained on a Co foil.

RESULTS

We first report the results obtained after testing the polycrystalline Co foil with a total surface area of 25 cm^2. In Fig. 2a the total product yield, i.e., the combined yield of (branched and linear) paraffins (P_n) and olefins (O_n), is plotted for various flows. Figure 2b shows the paraffin-to-olefin ratio, P_n/O_n, as a function of chain length. Except for C_1 and C_2 the yield decreases exponentially with carbon number. Figure 2 shows that the yield is unaffected by the flow rate, whereas P_n/O_n decreases with increasing flow rate.

Next we report the results obtained after testing the 2-in. SiO_2 wafer covered with cobalt particles. The overall product yields for three different flow rates are shown in Fig. 3a. The corresponding paraffin/olefin ratios are given in Fig. 3b. For Co/SiO_2 the total product distribution does not show a continuous exponential decrease with carbon number as was the case for the Co foil. The paraffin/olefin ratios are much lower than for the case of the Co foil and show a weaker dependence on flow.

To obtain more insight into the role of secondary reactions we have done some additional cofeeding experiments. Hexene and hexadecane were cofed with the syngas feed. Over the Co foil, hexene was hydrogenated. The fraction of the cofed hexene that was hydrogenated did not differ from the hydrogenated fraction of the synthesized hexene. No hydrogenolysis of reinsertion was observed. Hexadecane was hydrogenolyzed to some extent.

On Co/SiO_2 the cofed hydrocarbons underwent different reactions. Here the hydrogenated fraction of the added hexene was much lower than for the synthesized hexene. Also no hydrogenolysis or reinsertion could be observed. Cofed hexadecane was hydrogenolyzed to some extent on Co/SiO_2.

DISCUSSION

In the Fischer–Trospch synthesis growing linear alkane chains are chemically bound to the surface. This bond can be broken either by β-hydrogen abstraction yielding an α-olefin, or by α-hydrogenation yielding an n-paraffin. The thus-formed hydrocarbons can undergo secondary reactions like hydrogenation, reinsertion, and hydrogenolysis. Hydrogenation will convert an olefin into a paraffin. This changes the paraffin-to-olefin ratio, but has no direct impact on the growth probability. Reinsertion of an α-olefin into the chain growth process, on the other hand, reverses the termination via β-dehydrogenation and will thus affect the net chain growth probability, α_n, defined as the yield of chains with carbon number $n + 1$ divided by the yield of chains with carbon number n. Hydrogenolysis of paraffins and olefins will reverse the growth process and will thus lead to a decrease in α_n. Previously it has been shown that the reinsertion rate (8) and the hydrogenation rate (3) increase exponentially with carbon number, since they depend on the olefin concentration in the physisorbed state, which increases exponentially with chain length due

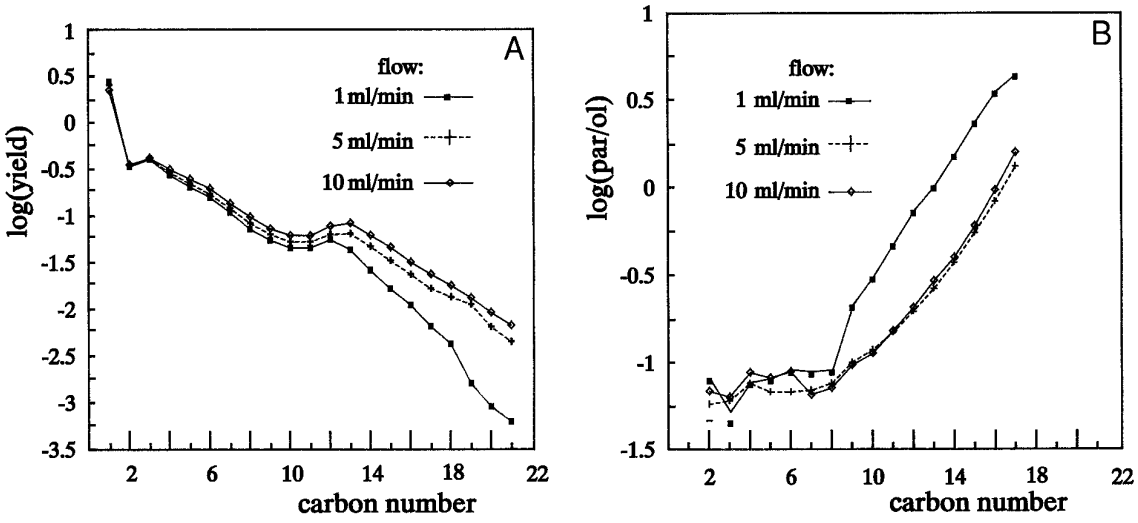

FIG. 3. (A) Total product yield (pmol/cm^2 · s) as a function of carbon number obtained for a 50-nm Co particles on a flat SiO_2 wafter (reduced at 573 K for 5 min) for three different flows, T = 493 K, H_2/CO = 2, P = 1 bar. (B) The corresponding paraffin-to-olefin ratios as a function of carbon number.

to a preferential physisorption of longer hydrocarbons at the surface of the catalyst (3, 4). For this study we have developed a model describing the impact of these chain-length-dependent secondary reactions on the product distribution of the FT reaction in the absence of diffusion limitations. This model is described in Appendix A. In the model we have investigated the impact of hydrogenation, reinsertion, and hydrogenolysis. This model will now be used to discuss the data.

Co Foil

A polycrystalline Co foil yields an ASF product distribution with $\alpha = 0.5$, as is shown in Fig. 2a. This suggests that reinsertion and hydrogenolysis do not play a major role. The paraffin-to-olefin ratio, on the other hand, strongly increases with chain length and decreases with increasing flow, showing that secondary hydrogenation does play a major role. These interpretations are confirmed by the cofeeding experiments. No measurable fraction of the cofed hexene was reinserted or hydrogenolyzed whereas it was hydrogenated to the same extent as the primary olefin product. A small fraction of the cofed hexadecane, however, was hydrogenolyzed, showing that for longer paraffins hydrogenolysis does play a role. The product distributions can be fitted with the model described in the Appendix. The resulting values for the secondary velocity rate constants obtained from model fitting are given in Table 1, reflecting the importance of hydrogenation and the absence of reinsertion.

Co/SiO$_2$

Cobalt particles on SiO_2 wafers yield product distributions which are drastically different from those obtained for a cobalt foil. In the first instance, the paraffin/olefin ratio, as shown in Fig. 3b, is up to two orders of magnitude lower than that obtained on a Co foil, indicating that hydrogenation hardly plays a role. This is also reflected by the hexene cofeeding experiment, which showed hardly any secondary hydrogenation. The product distributions deviate significantly from ASF, as shown in Fig. 3a. This indicates that reinsertion and/or hydrogenolysis plays a role as previously discussed. The deviation becomes even more clear from Fig. 5b where the net chain growth probability, α_n, is plotted versus carbon number, α_n shows a strong variation with n. For $4 \leq n \leq 9$, α_n slightly decreases with n. For $10 \leq n \leq 13$, α_n strongly increases to values even above 1. Finally the net growth probability dips again to values around 0.6–0.8, depending on the flow. Although the chain length dependence of α_n suggests that reinsertion

TABLE 1

Values Used to Fit the Experimentally Observed Product Distributions

	Co foil	Co/SiO_2
T^{par}	0.02	0.018
T^{ol}	0.49	0.2
R_0^i	—	0.015
k^i	—	1×10^{-5}
R_0^h	7×10^{-4}	—
k^h	0.001	—
k^a	—	1×10^{-4}
R_0^g	—	1×10^{-4}
β	—	0.5

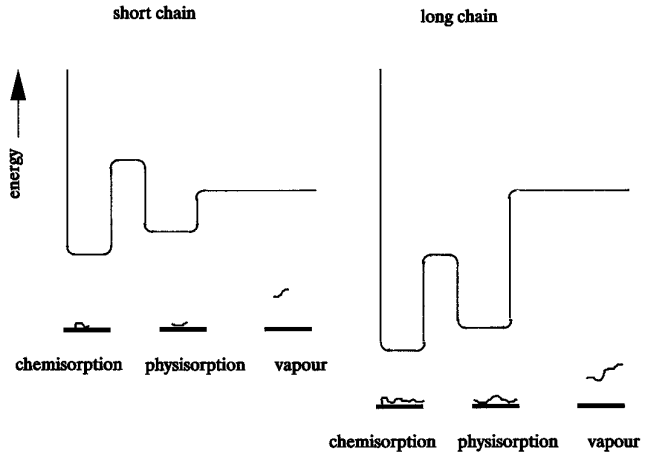

FIG. 4. A schematic diagram for the energy as a function of reaction coordinate for reinsertion of both a short and a long olefin.

does play a significant role already for $n = 6$, cofed hexene is not reinserted to a measurable amount. Thus the reinsertion rate of cofed α-olefins was found to be much lower than expected at first on the basis of the changes in the net growth probability. Also the dependence of the product distribution on the flow shows an anomalous behavior. It is expected that secondary reactions decrease with increasing space velocity as has been observed for hydrogenation on a cobalt foil. Thus for the case of Co/SiO_2 the deviations from the ASF distribution are expected to vanish with increasing flow. However, the non-ASF behavior up to C_{13} is virtually independent of the flow. This seeming contradiction between the chain-length dependence of α_n and the cofeeding as well as variable flow data suggests that part of the chain-length-dependent reinsertion does not take place via the vapor phase. Actually, this is not very surprising, since it is suggested in the literature that there is a clear distinction between a growth site and a hydrogenation or hydrogenolysis site (67). Thus, to be hydrogenated, an α-olefin has to leave its site of creation and desorb in order to readsorb at a hydrogenation site. This results in the flow dependence as observed for hydrogenation on a Co foil. However, reinsertion into the chain growth occurs at a growth site. Thus, to be reinserted, the α-olefin does not necessarily have to leave its site of creation. After breaking the chemical bond with the surface, the produced α-olefin is still physisorbed and therefore has a chance to chemisorb again prior to desorption. Thus physisorption acts as an ''umbilical cord'' between the α-olefin and the growth site. The strength of the physisorptive bond will increase with chain length. Thus the activation energy for desorption to the vapor phase will increase with chain length, whereas the activation energy to chemisorb at the growth site will stay the same. This is exemplified in Fig. 4 by schematic diagrams. For a short hydrocarbon the activation barrier for chemisorption will be higher than for desorption and therefore a short chain has a low probability of reinsertion prior to desorption, which will allow equilibration between the physisorbed and vapor phase. However, for the case of long chains, desorption becomes the most difficult process resulting in a high probability of reinsertion prior to desorption. Therefore no equilibration between the physisorbed and vapor phase will occur for the long olefins. Since the thus reinserted olefins have never been released to the vapor phase, the umbilical cord mechanism will be essentially independent of flow. The umbilical cord mechanism also explains the difference between reinsertion of α-olefins cofed in the vapor phase and reinsertion of the primary α-olefin product.

The model described in Appendix A is now used to obtain some insight into the extent of reinsertion, hydrogenolysis, and hydrogenation.

First the effect of reinsertion and hydrogenation will be considered. To investigate its impact on both $(P_n + O_n)$ and α_n, Eqs. [A1]–[A7] have to be used. In these equations, R_0^{i}, R_0^{h}, k^{i}, k^{h}, T^{par}, and T^{ol} are variables. At low carbon numbers secondary reactions hardly affect the product distribution, which is reflected by the observed n-independence of the paraffin/olefin selectivity at low carbon numbers. Therefore, we can directly determine T^{par} and T^{ol} from the growth probability and the paraffin/olefin selectivity at low carbon numbers. Using these values $R_0^{\mathrm{i}}, R_0^{\mathrm{h}}$, k^{i}, and k^{h} can then be used to fit the product distribution at higher carbon numbers, where reinsertion plays a dominant role. The fit which can be obtained in this way is shown in Fig. 5. At low values of the carbon number the desorption rate, R_n^{des}, is very high and thus α_n does not differ from α. For $6 \leq n \leq 9$ an increasing number of the primary α-olefins is being reinserted, thus $T_{n+1}^{\mathrm{ol}} < T_n^{\mathrm{ol}}$, causing a small decrease in α_n in this regime. For $n > 15$ almost all the α-olefins are being reinserted thus $T_n^{\mathrm{ol}} = T_{n+1}^{\mathrm{ol}} = 0$, causing an increase of α_n up to $(1 - T_n^{\mathrm{par}})$. As can be observed in Fig. 5, reinsertion of olefins can only partly explain the observed chain length dependence of the net chain growth probability, namely the small decrease for $n \leq 9$ and only partly the increase at $n > 9$. To obtain a better fit we also have to consider the effect of hydrogenolysis on the product distribution.

Cobalt is an efficient catalyst for the hydrogenolysis of hydrocarbons in an H_2 atmosphere (53). The hydrogenolysis rate will drop severely with CO pressure, but several studies have shown that under FT synthesis conditions a considerable amount of the produced α-olefins is still hydrogenolyzed (12, 18, 21, 23, 32, 40, 44, 46, 48, 56). However, since at first the growth probability increases with carbon number, we can assume that reinsertion of α-olefins occurs much faster than hydrogenolysis. Thus, only a negligibly small fraction of the primary α-olefin

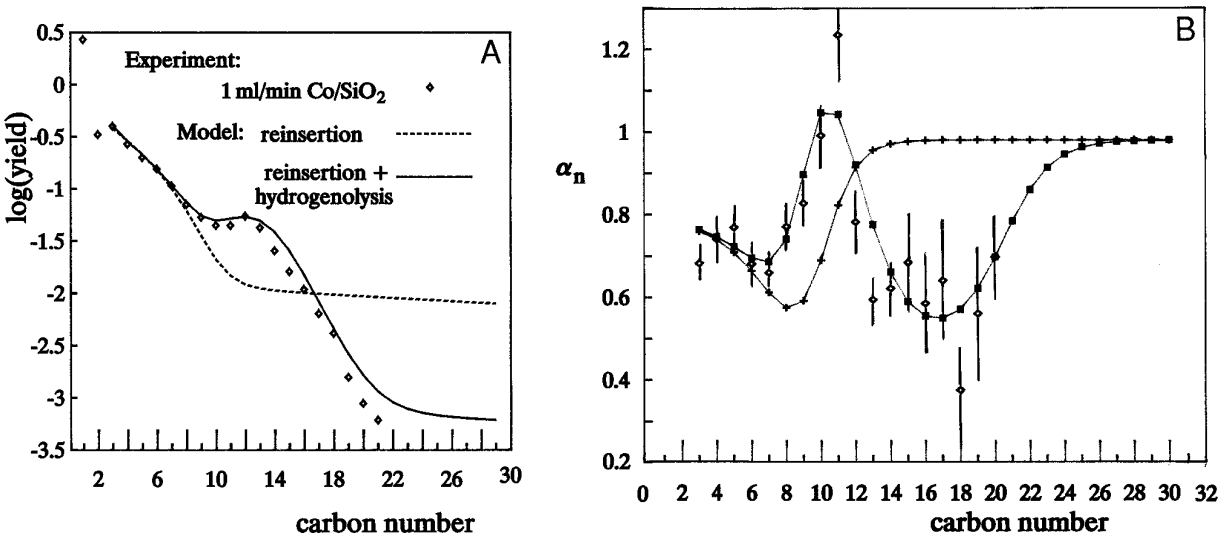

FIG. 5. (A) Fits to the total product yield of 50-nm Co particles on a flat SiO_2 wafer for $\Phi = 1$ STP ml/min using the model described in the Appendix. (B) The experimentally found values of α_n obtained for 50-nm Co particles on a flat SiO_2 wafer ($\diamond$) ($\Phi = 1$ STP ml/min) and fits using the olefin reinsertion model and the olefin reinsertion/paraffin hydrogenolysis model described in the Appendix.

product will be hydrogenolyzed. Paraffins on the other hand are not consumed by reinsertion and can therefore fully participate in hydrogenolysis. Thus the overall impact of hydrogenolysis is expected to be determined by the hydrogenolysis of the paraffins and we will neglect the impact of olefin hydrogenolysis. In the literature hardly any information can be found on the hydrogenolysis of paraffins during FT synthesis, although there are some indications that it can occur (18, 32, 61). These indications are verified by our hexadecane cofeed studies where hydrogenolysis was observed even under FT synthesis conditions.

Equations [A8]–[A12] can be used to investigate the impact of hydrogenolysis on both P_n and α_n. To fit the data in Fig. 5 effectively two extra fitting parameters can now be used, namely the velocity constant for adsorption at a hydrogenolysis site, k^a ($m \cdot s^{-1}$), and the reversed growth probability, β. A resulting fit is shown in Fig. 5. As can be observed, the model can reproduce the data well.

Although all the product spectra can be fitted separately with the model described in Appendix A, it does not give a fully correct description of the impact of the gas flow, Φ, on the C_{10}^+ product yield. This is not surprising, since the hydrogenolysis model in the appendix is oversimplified. Several uncertainties have been tacitly ignored. Hydrogenolysis of olefins has not been taken into account. Hardly anything is known about the hydrogenolysis of long hydrocarbons under FT synthesis; e.g., does hydrogenolysis yield paraffins or also a small fraction of α-olefins which can be reinserted again? The dependence of k^{sec} on the conversion has been neglected (3). In view of these uncertainties, the fit values for the C_{10}^+ product yield, i.e., the parameters for the hydrogenolysis, should not be taken too seriously. However, the experimentally obtained product spectra, the cofeeding experiments, and the product distributions obtained with the model all show conclusively that the non-ASF behavior is caused by chain-length-dependent α-olefin reinsertion and hydrogenolysis reactions.

Recently Iglesia *et al.* have shown to what extent chain-length-dependent α-olefin reinsertion influences the total product distribution. This extent was only partly dependent on the catalyst contact time, suggesting that transport limitation of olefins in the catalyst pores played a role. Thus the authors attributed the chain-length dependence to the diffusion of the olefins out of the catalyst pores. In a recent study on secondary hydrogenation during FT synthesis, we have shown that the same chain-length dependence is observed on flat model catalysts where transport limitations do not play a role at all (3). Thus the chain-length dependence was attributed by us to a preferential physisorption of longer hydrocarbons at the surface of the catalyst. In this study we have shown that α-olefin reinsertion on a flat model catalyst shows the same chain-length dependence. In contrast to hydrogenation, but in agreement with the observations by Iglesia, the extent of reinsertion only partly depends on the catalyst contact time. In our system this cannot be caused by transport limitations, but has been attributed to an umbilical cord mechanism as has been discussed above.

The umbilical cord mechanism plays a role when an α-olefin, which is physiorbed next to a growth site, has a reasonable chance to be reinserted prior to desorption. Reinsertion of vapor phase olefins increases with contact time/conversion. Our experiments have been done at very low conversions making reinsertion from the vapor phase

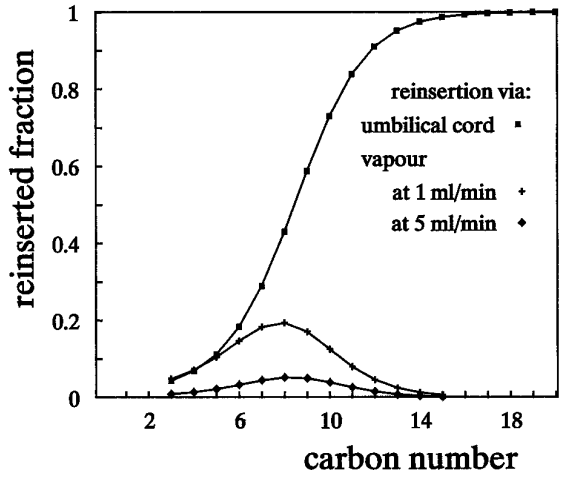

FIG. 6. The fraction of the primary olefin product reinserted via the umbilical cord mechanism, i.e., without desorption to the vapor phase (■), and reinserted via desorption to the vapor phase for $\Phi = 1$ STP ml/min (+) and for $\Phi = 5$ STP ml/min (•).

unlikely. As a result the umbilical cord mechanism is the main mode of reinsertion especially for long olefins. This is reflected by Fig. 6, which shows the fraction of the primary α-olefin product reinserted via the umbilical cord mechanism, i.e., prior to desorption to the vapor phase, and the fraction which has been reinserted after desorption to and readsorption from the vapor phase. The separation into these two processes has been obtained from the previously discussed fit to the data. As expected, Fig. 6 shows that especially for the case of small catalyst contact times and high carbon numbers, most of the reinserted α-olefins have never left the surface zone. For the case of high carbon numbers all the primary α-olefin product is reinserted by the umbilical cord mechanism, which means that the long α-olefins have a negligible chance to desorb into the vapor phase. Once they have reached a critical chain length they will reinsert continuously at the same growth site until they finally terminate as a paraffin. Since paraffins are not prone to reinsertion, they will eventually desorb to the vapor or liquid phase. Shorter α-olefins have a chance to break the umbilical cord prior to reinsertion. Once in the vapor phase these olefins have only a small chance of being reinserted again, as is reflected by the negligible small reinserted fraction of cofed olefins. For Co/SiO_2 this fraction is much smaller than, e.g., the hydrogenated fraction of cofed α-olefins on a Co foil. Apparently the growth sites cover only a small part of the surface. This is in agreement with other studies showing that less than 0.5% of the exposed metal surface atoms are occupied by growing chains (68).

On cobalt, hydrogenolysis will shorten hydrocarbons by successive demethylation. Since hydrogenolysis is a secondary reaction, its rate will increase exponentially with chain length. In conjunction with reinsertion, this causes the strong fluctuations of the net growth probability as shown in Fig. 5b. Leafing through the FT literature one can find many product distributions with a striking similarity to the sigmoid product distribution predicted by the reinsertion/hydrogenolysis model shown in Fig. 5a (69–73). In all these cases a drop in the growth probability around $n = 15$ has been observed, which has mostly been attributed to product retentions and condensations. Note, however, that retention or condensation cannot cause the observed sigmoid curves or the differences between olefins and paraffins. We suggest that all these sigmoid curves are most probably caused by a chain-length-dependent hydrogenolysis. Recently, Madon and Iglesia were the first to attribute sigmoid product distributions to hydrogenolysis (60).

Due to the chain-length dependence the hydrogenolysis is very selective. The C_{16}^{+} hydrocarbons are almost fully hydrogenolyzed to products in the C_{11}–C_{16} region, whereas the C_{11}- products are hardly hydrogenolyzed at all. Thus due to this chain-length-dependent hydrogenolysis, the middle distillate yield is increased. Previously Foley *et al.* have thought of the possibility of increasing the selectivity toward middle distillates by hydrogenolysis. To this end they have proposed a combined FT and hydrogenolysis catalyst (74). They did not realize that hydrogenolysis under FT reaction conditions is strongly chain-length-dependent due to competitive physisorption. Thus to introduce the necessary chain-length dependence they have investigated the feasibility of incorporating the catalyst in a carbon molecular sieve. Transport limitation through this sieve would then induce the favorable chain length dependence. However, in view of the present study this carbon molecular sieve is expected to be superfluous. Although the middle distillate yield can be increased by hydrogenolysis, this does not seem economically attractive, since it is done by successive demethylation causing an increase of the methane make. Separate hydrocracking of heavy paraffins, as is currently done in the Shell Middle Distillate Synthesis, remains a better alternative (75).

So far we have discussed the impact and flow-dependence of secondary reactions. It has been shown that hydrogenation only gives rise to a change in the paraffin-to-olefin ratio and is directly dependent on the flow, whereas reinsertion and hydrogenolysis give rise to non-ASF product distribution and are not directly dependent on the flow. It has been shown that Co foil and Co/SiO_2 yield completely different product distributions mainly due to a difference in secondary reaction rates. So far we have not discussed the essential difference in these systems that causes this behavior. To this end we will discuss dispersion effects mentioned in the literature.

A large number of papers has been published on the influence of particle size on the catalytic properties of supported metals (76). When the particle size has no effect

on the catalytic properties, the reaction is called facile or structure insensitive. If particle size effects are observed, the reaction is said to have a sympathetic structure sensitivity in case the activity increases with dispersion and an antipathetic structure sensitivity in case the activity decreases with dispersion. Structure sensitivity can be caused by electronic effects or by geometric effects. Electronic effects are caused by a change of the electron energy levels, coming from the band structure of a bulk metal eventually splitting up into the orbitals of a single atom. It can be easily shown that electronic effects are only expected to play a role at particle diameters smaller than 2 nm. Geometric effects can already play a role at much larger diameters. For metal clusters with a diameter of 50 nm or less the fraction of edge and corner atoms will be substantial with respect to face atoms (77). Thus if the catalytic properties of edge and corner atoms differ from those of face atoms, a structure sensitivity will be observed for a particle size of 50 nm or less.

In the past 10 years several studies showed strong dispersion effects for the hydrogenation of CO on group VIII metals. Most of these studies found a decrease of the CO turn-over-number (TON) with dispersion (78–89). This decrease starts at particle diameters as large as 100 nm. Fewer studies are known that deal with the impact of dispersion on the selectivity, and the conclusions of these few studies are even contradictory, since both a decrease (86–88) and an increase (90) of the average carbon number with dispersion have been reported. A closer investigation revealed that the above mentioned effects were not directly caused by the dispersion of the metal, but were due to the resulting change in the extent of reduction (91–95). At the same extent of reduction, no significant variations of activity and selectivity with dispersion were observed. Thus one concluded that the metal is the active phase and that oxidized particles show no activity at all. It has been suggested by Iglesia *et al.* that the intrinsic performance of cobalt does not depend on the nature of support or promoters.

Practically all studies mentioned above have investigated the impact of dispersion on the primary chain growth reaction. The influence on secondary reactions of primarily produced hydrocarbons has, to our knowledge, previously only been discussed by Iglesia *et al.* (94), who investigated the effect of dispersion for both Co and Ru on the product spectrum up to C_{50}. Small selectivity changes were observed due to a variation in α-olefin reinsertion. This variation was not attributed to a change of reactivity of the cobalt with dispersion, but to the variation of the physical structure of the support and the density of exposed metal atoms within pellets with dispersion.

Hardly anything is known on dispersion effects for secondary reactions during FT synthesis, but the impact on both hydrogenolysis and hydrogenation of hydrocarbons in an H_2 atmosphere has been thoroughly investigated. Thus it is known that hydrogenation of hydrocarbons on group VIII metals is a facile reaction (76). Hydrogenolysis of linear hydrocarbons on the other hand is structure sensitive, showing an increase of activity with a decrease of the particle diameter to a few nanometers and a subsequently activity decrease for smaller particles (76).

In view of these studies we interpret that the difference observed in the catalytic behavior of the Co-foil and the Co particles is caused by geometric effects, i.e., an increased amount of corner and edge atoms. These atoms will have another reactivity affecting their catalytic behavior. To obtain more information we have set out to investigate the impact of the dispersion and degree of reduction by testing various model catalysts with different Co-particle sizes and by using X-ray photoelectron spectroscopy to determine the degree of oxidation. We intend to report the outcome of this study in a future publication.

CONCLUSIONS

Chain-length-dependent secondary reactions strongly influence the product spectrum for flat FT model catalysts:

—For a Co foil the main secondary reaction is the hydrogenation of the primary α-olefin product. This causes an exponential increase in the paraffin-to-olefin ratio with chain length but does not influence the total product spectrum.

—For 50-nm Co particles on a SiO_2 wafer, reinsertion of α-olefins in the chain growth process is the major secondary reaction. In contrast to hydrogenation, reinsertion is only partly dependent on the catalyst contact time, showing that a fraction of the primary α-olefin product is reinserted prior to desorption to the vapor phase. The physisorption bond to the surface acts as an umbilical cord, causing the α-olefin to remain for some time next to its site of creation, so that it can reinsert prior to desorption.

—Under FT synthesis conditions long hydrocarbons can be hydrogenolyzed via successive demethylation to shorter hydrocarbons.

—Chain-length-dependent reinsertion and hydrogenolysis strongly influence the total product distribution eventually leading to sigmoid distributions with a high selectivity to middle distillates. The product distributions can be fitted with a simple model.

—The difference in catalytic behavior between a Co foil and Co/SiO_2 is ascribed to a difference in the amount of edge atoms affecting the degree of reactivity.

APPENDIX A

In this appendix we will develop a model describing the impact of chain-length-dependent secondary reactions on the product distribution of a primary FT reaction.

Secondary gas–surface reaction velocity constants depend on the hydrocarbon residence time in the physisorbed state, which increases exponentially with chain length (3, 4). In the absence of transport limitations, the chain-length–dependent (n) gas–surface secondary reaction velocity constant, $k_n^{\text{sec}}(\text{m}\cdot\text{s}^{-1})$, can be given by (3)

$$k_n^{\text{sec}} = k^{\text{sec}} \cdot \frac{R^{\text{sec}}}{R^{\text{sec}} + R_n^{\text{des}}}, \qquad [A1]$$

where k^{sec} is the gas–surface velocity constant ($\text{m}\cdot\text{s}^{-1}$) for physisorption near a secondary reaction site. Note that both k^{sec} and k_n^{sec} are velocity constants for the reaction of vapor phase molecules. k^{sec} is the gas–surface velocity constant for adsorption, whereas k_n^{sec} is that for a secondary reaction. Equation [A1] says that k_n^{sec} is only a fraction of k^{sec}. For reasons of simplicity we have assumed that k^{sec} is n independent. Later on we will further comment on the implications of this assumption. Once physisorbed, molecules undergo a secondary reaction with reaction rate R^{sec} (s^{-1}) or they can desorb back to the vapor phase with desorption rate R_n^{des}. In a previous study at $T = 493$ K we have found that the latter decreases with n, $R_n^{\text{des}} \sim n \cdot e^{-(0.75\pm0.15)n}$, when transport limitations do not play a role (3). Thus we can write $k_n^{\text{des}} = R_0^{\text{sec}}/(R_0^{\text{sec}} + n \cdot e^{-(0.75\pm0.15)n})$, where R_0^{sec} is a dimensionless constant.

As secondary reactions for primary produced α-olefins, we first consider only hydrogenation and reinsertion. The fraction of the primary α-olefin product that will undergo a secondary reaction, F_n^{sec}, can be written as

$$F_n^{\text{sec}} = \frac{k_n^{\text{sec}} \cdot A}{\Phi + (k_n^{\text{i}} + k_n^{\text{h}}) \cdot A}, \qquad [A2]$$

where A is the surface area of the catalyst (m^2), Φ is the flow ($\text{m}^3\cdot\text{s}^{-1}$), and k_n^{i} and k_n^{h} are, respectively, the reinsertion and hydrogenation velocity constants ($\text{m}\cdot\text{s}^{-1}$).

Hydrogenation will turn an α-olefin into a paraffin and thus will lead to an increase of the net termination probability as a paraffin with chain length n, T_n^{par}, which is exactly offset by the decrease in the net termination probability as an α-olefin with chain length n, T_n^{ol}. This will not directly result in a change of the net growth probability. Reinsertion of an α-olefin into the chain growth mechanism reverses the termination by β-dehydrogenation leading to a decrease in T_n^{ol} and thus to an increase of the net growth probability. In agreement with the literature this study shows that there is a clear distinction between a growth site and a hydrogenation site. Thus for secondary hydrogenation an α-olefin has to leave its site of creation and desorb to readsorb at a hydrogenation site. This results in the Φ dependence of Eq. [A2]. However, for reinsertion Eq. [A2] has to be modified, since in order to be reinserted the α-olefin does not necessarily have to leave its site of birth. After breaking the chemical bond with the surface, the produced α-olefin is still physisorbed. The physisorbed molecule has a chance to chemisorb again at its site of birth prior to desorption. Thus due to this umbilical cord the probability of an alkyl chain to escape via β-dehydrogenation changes. This change is determined by the rate of reinsertion of the physisorbed molecule versus its desorption rate. Thus T_n^{ol} and T_n^{par} can be written as

$$T_n^{\text{ol}} = T^{\text{ol}} \cdot \left(\frac{R_n^{\text{des}}}{R^{\text{i}} + R_n^{\text{des}}}\right) \cdot \frac{\Phi}{\Phi + (k_n^{\text{i}} + k_n^{\text{h}}) \cdot A} \qquad [A3]$$

$$T_n^{\text{par}} = T^{\text{par}} + T^{\text{ol}} \cdot \left(\frac{R_n^{\text{des}}}{R^{\text{i}} + R_n^{\text{des}}}\right) \cdot \left(\frac{k_n^{\text{h}} \cdot A}{\Phi + (k_n^{\text{i}} + k_n^{\text{h}}) \cdot A}\right), \qquad [A4]$$

where R^{i} is the reinsertion rate in s^{-1}. Note that the n dependence of the umbilical cord mechanism will differ from the n dependence of the secondary reactions going via the vapor phase if k^{sec} does depend on n.

The net production per m^2 of catalyst per second ($\text{m}^{-2}\cdot\text{s}^{-1}$) of both olefins and paraffins with chain length n, O_n, and P_n can be written for $n \geq 3$ as

$$O_n = T_n^{\text{ol}} \cdot I_2 \cdot \prod_{m=2}^{n-1} (1 - T_m^{\text{par}} - T_m^{\text{ol}}) \qquad [A5]$$

$$P_n = T_n^{\text{par}} \cdot I_2 \cdot \prod_{m=2}^{n-1} (1 - T_m^{\text{par}} - T_m^{\text{ol}}), \qquad [A6]$$

where I_2 is a constant.

So far we have dealt with the effect of hydrogenation and reinsertion of α-olefins. Now we will consider hydrogenolysis.

We assume that under FT reaction conditions the reinsertion of α-olefins proceeds so much faster than the hydrogenolysis that practically nothing of the primary α-olefin product will have a chance to be hydrogenolyzed. Thus for reasons of simplicity we will neglect the hydrogenolysis of olefins. Paraffins on the other hand cannot be reinserted and therefore even at very low rates hydrogenolysis can have a notable impact on its product distribution. To investigate this, we first write an expression for the physisorption probability of a paraffin with chain length n next to a hydrogenolysis site, F^{ads},

$$F^{\text{ads}} = \frac{k^{\text{a}} \cdot A}{\Phi + k^{\text{a}} \cdot A}, \qquad [A7]$$

where k^{a} is the velocity constant for physisorption next to

a hydrogenolysis site ($m \cdot s^{-1}$). Once physisorbed near a hydrogenolysis site the chance to chemisorb at that site, P_n^g, can be written as

$$P_n^g = \frac{R^g}{R^g + R_n^{des} \cdot (1 - F^{ads})}, \quad [A8]$$

where R^g is the chemisorption rate at the hydrogenolysis site in s^{-1}.

Hydrogenolysis on cobalt occurs by a successive demethylation of the end carbon atom [54], which partly causes the above ASF yield of CH_4 (18, 32, 44, 46, 57). Hydrogenolysis by successive demethylation is a reversed chain growth reaction for which we can define a reversed growth probability, β, as

$$\beta = \frac{R^{depol}}{R^{depol} + R^{esc}}, \quad [A9]$$

where R^{depol} is the depolymerization rate (s^{-1}) and R^{esc} is the rate of escape from the hydrogenolysis site (s^{-1}). A paraffin that succeeds in escaping from the hydrogenolysis site also has a chance of being trapped again, and thus the net chain-length-dependent reversed growth probability, β_n, can be written as

$$\beta_n = \frac{R^{depol}}{R^{depol} + R^{esc} \cdot (1 - P_n^g)}. \quad [A10]$$

The fraction of paraffins with chain length m, that is hydrogenolyzed to paraffins with chain length n ($<m$), $F_{m,n}$, can be written as

$$F_{m,n} = F_m^{ads} \cdot (1 - \beta_n) \cdot \prod_{j=n+1}^{m} \beta_j. \quad [A11]$$

Due to hydrogenolysis P_n will change to $P'_n(m^{-2} \cdot s^{-1})$:

$$P'_n = (1 - F^{ads}) \cdot P_n + F^{ads} \cdot (1 - \beta_n) \cdot P_n + \sum_{m=n+1}^{\infty} F_{m,n} \cdot P_m$$

$$= (1 - F^{ads} \cdot \beta_n) \cdot P_n + \sum_{m=n+1}^{\infty} F_{m,n} \cdot P_m. \quad [A12]$$

APPENDIX B: NOMENCLATURE

A	Surface area of the catalyst (m^2).
F_n^{sec}	Fraction of the primary α-olefin product undergoing a secondary reaction.
F^{ads}	Physisorption probability of a paraffin next to a hydrogenolysis site.
$F_{m,n}$	Fraction of paraffins with chain length m, that is hydrogenolyzed to paraffins with chain length n ($<m$).
I_2	Constant.
k_n^{sec}	Chain-length-dependent secondary reaction velocity constant ($m \cdot s^{-1}$).
k_n^i	Chain-length-dependent reinsertion velocity constant ($m \cdot s^{-1}$).
k_n^h	Chain-length-dependent hydrogenation velocity constant ($m \cdot s^{-1}$).
k^{sec}	Velocity constant for physisorption near a secondary reaction site ($m \cdot s^{-1}$).
k^i	Velocity constant for physisorption near a growth site ($m \cdot s^{-1}$).
k^h	Velocity constant for physisorption near a hydrogenation site ($m \cdot s^{-1}$).
k^a	Velocity constant for adsorption at a hydrogenolysis site ($m \cdot s^{-1}$).
n	Carbon number.
Q_n	Net production of olefins with chain length n if reinsertion of olefins is taken into account ($m^{-2} \cdot s^{-1}$).
P_n	Net production of paraffins with chain length n if reinsertion of olefins is taken into account ($m^{-2} \cdot s^{-1}$).
P'_n	Net production of paraffins with chain length n if both olefin reinsertion and paraffin hydrogenolysis are taken into account ($m^{-2} \cdot s^{-1}$).
P_n^g	Probability to chemisorb at a hydrogenolysis site.
R^{depol}	Depolymerisation rate (s^{-1}).
R^{esc}	Escape rate from a hydrogenolysis site (s^{-1}).
R^g	Chemisorption rate at a hydrogenolysis site (s^{-1}).
R^h	Hydrogenation rate (s^{-1}).
R^i	Reinsertion rate (s^{-1}).
R^{sec}	Secondary reaction rate (s^{-1}).
R_0^{sec}	Constant to fit fraction of olefins undergoing a secondary reaction.
R_0^h	Constant to fit hydrogenated fraction of olefins.
R_0^i	Constant to fit reinserted fraction of olefins.
R_n^{des}	Chain-length-dependent desorption rate (s^{-1}).
T	Temperature (K).
T^{par}	Termination probability by α-hydrogenation.
T^{ol}	Termination probability by β-hydrogenation.
T_n^{par}	Net termination probability as a paraffin with chain length n.
T_n^{ol}	Net termination probability as an α-olefin with chain length n.
α	Chain growth probability.
α_n	Net chain growth probability.
β	Reversed growth probability.
β_n	Net chain-length-dependent reversed growth probability.
Φ	Flow ($m^3 \cdot s^{-1}$).

REFERENCES

1. Henrici-Olive, G., and Olive, S., *in* "The Chemistry of the Metal-Carbon Bond" (F. R. Hartley and S. Patai, Eds.), Vol. 3, Chap. 9. Wiley, New York, 1985.
2. Madon, R. J., Reyes, S. C., and Iglesia, E., *J. Phys. Chem.* **95,** 7795 (1991).
3. Kuipers, E. W., Vinkenburg, I. H., and Oosterbeek, H., *J. Catal.* **152,** 137 (1995).
4. Komaya, T., and Bell, A. T., *J. Catal.* **146,** 237 (1994).
5. Pichler, H., Schulz, H., and Elstner, M., *Brennst. Chem.* **48,** 78 (1967).
6. Dictor, R. A., and Bell, A. T., *J. Catal.* **97,** 121 (1986).
7. Gaube, J., and Hochstadt, G., *Chem. Ing. Tech.* **50,** 627 (1978).
8. Iglesia, E., Reyes, S. C., and Madon, R. J., *J. Catal.* **129,** 238 (1991).
9. Jordan, D. S., and Bell, A. T., *J. Phys. Chem.* **90,** 4797 (1986).
10. Jordan, D. S., and Bell, A. T., *J. Catal.* **107,** 338 (1987).
11. Jordan, D. S., and Bell, A. T., *J. Catal.* **108,** 63 (1987).
12. Krishna, K. R., and Bell, A. T., *Catal. Lett.* **14,** 305 (1992).
13. Copperthwaite, R. G., Hutchings, G. J., van der Riet, M., and Woodhouse, J., *J. Ind. Eng. Chem. Res.* **26,** 869 (1987).
14. Matsumoto, D. K., and Satterfield, C. N., *Energy Fuels* **3,** 287 (1989).
15. Satterfield, C. N., and Stenger, H. G., *Ind. Eng. Chem. Prod. Res. Dev.* **23,** 26 (1984).
16. Satterfield, C. N., Huff, G. A., and Summerhayes, R., *J. Catal.* **80,** 486 (1983).
17. Schulz, H., van Steen, E., and Claeys, M., *Catal. Lett.* in press.
18. Pichler, H., and Schulz, H., *Chem. Ing. Tech.* **42,** 1162 (1970).
19. Barrault, J., Forquy, C., and Perrichon, V., *J. Mol. Catal.* **17,** 195 (1982).
20. Dwyer, D. J., and Somorjai, G. A., *J. Catal.* **56,** 249 (1979).
21. Eidus, Y. T., *Russ. Chem. Rev.* **36,** 338 (1967).
22. Adesina, A. A., Hudgins, R. R., and Silverston, P. L., *Appl. Catal.* **62,** 295 (1990).
23. Kobori, Y., Yamasaki, H., Naito, S., Onishi, T., and Tamaru, K., *Chem. Soc. Faraday Trans. 1* **78,** 1473 (1982).
24. Pichler, H., Schulz, H., and Kuhne, D., *Brennst. Chem.* **49,** 344 (1968).
25. Snel, R., and Espinoza, R. L., *J. Mol. Catal.* **54,** 119 (1989).
26. Ekerdt, J. G., and Bell, A. T., *J. Catal.* **62,** 19 (1980).
27. Tau, L. M., Dabbagh, H. A., and Davis, B. H., *Energy Fuels* **4,** 94 (1990).
28. Iglesia, E., Reyes, S. C., Madon, R. A., and Soled, S. L., *Adv. Catal.* **39,** 221 (1993).
29. Smith, D. F., Hawk, C. O., and Golden, P. L., *J. Am. Chem. Soc.* **52,** 3221 (1930).
30. Herrington, E. F., *Chem. Ind.* **65,** 346 (1946).
31. Morris, S. R., Moyes, R. B., and Wells, P. B., *J. Catal.* **96,** 23 (1985).
32. Schulz, H., Rao, B. R., and Elstner, M., *Erdoel Kohle* **23,** 651 (1970).
33. Hall, K. W., Kokes, R. J., and Emmett, P. H., *J. Am. Chem. Soc.* **82,** 1027 (1960).
34. Costa, J. L., Noels, A. F., Demonceau, A., and Hubert, A. J., *J. Catal.* **105,** 1 (1987).
35. Kummer, J. T., and Emmett, P. H., *J. Am. Chem. Soc.* **75,** 5177 (1953).
36. Blyholder, G., and Emmett, P. H., *J. Phys. Chem.* **63,** 962 (1959).
37. Blyholder, G., and Emmett, P. H., *J. Phys. Chem.* **64,** 470 (1960).
38. Kokes, R. J., Hall, W. K., and Emmett, P. H., *J. Am. Chem. Soc.* **79,** 2989 (1957).
39. Kummer, J. T., Podgurski, H. H., Spencer, W. B., and Emmett, P. H., *J. Am. Chem. Soc.* **73,** 564 (1951).
40. Molina, W., Perrichon, V., Sneeden, R. P. A., and Turlier, P., *React. Kinet. Catal. Lett.* **13,** 69 (1980).
41. Pijolat, M., and Perrichon, V., *Appl. Catal.* **13,** 321 (1985).
42. Bianchi, D., Tau, L. M., Borcar, S., and Bennett, C. O., *J. Catal.* **84,** 358 (1983).
43. Henrici-Olive, G., and Olive, S., *Angew. Chem. Int. Ed. Engl.* **15,** 136 (1976).
44. Snel, R., and Espinoza, R. L., *J. Mol. Catal.* **54,** 103 (1989).
45. Snel, R., and Espinoza, R. L., *J. Mol. Catal.* **43,** 237 (1987).
46. Snel, R., and Espinoza, R. L., *C_1 Mol. Chem.* **1,** 349 (1986).
47. Mims, C. A., Krajewski, J. J., and Rose, K. D., *Catal. Lett.* **7,** 119 (1990).
48. Percy, L. T., and Walter, R. I., *J. Catal.* **121,** 228 (1990).
49. Boelee, J. H., Custers, J. M. G., and van der Wiele, K., *Appl. Catal.* **53,** 1 (1989).
50. Stenger, H. G., and Satterfield, C. N., *Ind. Eng. Chem. Prod. Res. Dev.* **24,** 411 (1985).
51. Novak, S., Madon, R. J., and Suhl, H., *J. Chem. Phys.* **74,** 6083 (1981).
52. Iglesia, E., Soled, S., and Fiato, R. A., *J. Catal.* **137,** 212 (1992).
53. Davis, S. M., and Somorjai, G. A., *in* "The Chemical Physics of Solid Surfaces and Heterogeneous Catalysis" (D. A. King and D. P. Woodruff, Eds.), Vol. 4, Chap. 7. Elsevier, Amsterdam, 1982.
54. Kikuchi, E., Tsurumi, M., and Morita, Y., *J. Catal.* **22,** 226 (1971).
55. Carter, J. L., Cusumano, J. A., and Sinfelt, J. H., *J. Catal.* **20,** 223 (1971).
56. Gibson, E. J., *Chem. Ind.* **21,** 649 (1957).
57. Kolbel, H., Ludwig, H. B., and Hammer, H., *J. Catal.* **1,** 156 (1962).
58. Olive, S., and Henrici-Olive, G., *in* "The Chemistry of the M–C Bond" (F. R. Hartley and S. Patai, Eds.), Wiley, New York, 1985.
59. Novak, S., and Madon, R. J., *Ind. Eng. Chem. Fundam.* **23,** 274 (1984).
60. Madon, R. J., and Iglesia, E., *J. Catal.* **149,** 428 (1994).
61. Kellner, C. S., and Bell, A. T., *J. Catal.* **70,** 418 (1981).
62. Kuipers, E. W., Laszlo, C., and Wieldraaijer, W., *Catal. Lett.* **17,** 71 (1993).
63. Doornkamp, C., Laszlo, C., Wieldraaijer, W., and Kuipers, E. W., *J. Mater. Res.* **10,** 411 (1995).
64. van den Berg, R., Groesbeek, N., Knoester, A., Chen, Z. X., and Kuipers, E. W., submitted for publication.
65. Lahtinen, J., Anraku, T., and Somorjai, G. A., *J. Catal.* **142,** 206 (1993).
66. Geerlings, J. J. C., Zonnevylle, M. C., and de Groot, C. P. M., *Surf. Sci.* **241,** 315 (1991).
67. Schulz, H., van Steen, E., and Claeys, M., *Catal. Lett.* to appear.
68. Mims, C. A., McCandlish, L. E., and Melchior, M. T., *Catal. Lett.* **1,** 121 (1988).
69. Schulz, H., *C_1 Mol. Chem.* **1,** 231 (1985).
70. Dictor, R. A., and Bell, A. T., *Appl. Catal.* **20,** 145 (1986).
71. Huff, G. A., and Satterfield, C. N., *J. Catal.* **85,** 370 (1984).
72. Donnelly, T. J., and Satterfield, C. N., *Appl. Catal.* **52,** 93 (1989).
73. Yates, I. C., and Satterfield, C. N., *Energy Fuels* **6,** 308 (1992).
74. Lafyatis, D. S., and Foley, H. C., *Chem. Eng. Sci.* **45,** 2567 (1990).
75. van den Burgt, M. J., van Leeuwen, C. J., del'Amico, J. J., and Sie, S. T., *in* "Methane Conversion" (D. M. Bibby *et al.,* Eds.), p. 473. Elsevier, Amsterdam, 1988.
76. Che, M., and Bennett, C. O., *Adv. Catal.* **36,** 55 (1989).
77. van Hardeveld, R., and Hartog, F., *Adv. Catal.* **22,** 75 (1972).
78. van Meerten, R. Z. C., Beaumont, A. H. G. M., van Nisselrooij, P. F. M. T., and Coenen, J. W. E., *Surf. Sci.* **135,** 565 (1983).
79. Bartholomew, C. H., Pannell, R. B., and Butler, J., *J. Catal.* **65,** 335 (1980).
80. Bhatia, S., Bakhshi, N. N., and Mathews, J. F., *Can. J. Chem. Eng.* **56,** 575 (1978).
81. King, D. L., *J. Catal.* **51,** 386 (1978).
82. Vannice, M. A., *J. Catal.* **40,** 129 (1975).
83. Elliott, D. J., and Lunsford, J. H., *J. Catal.* **57,** 11 (1979).
84. Dalla Betta, R. A., Piken, A. G., and Shellef, M., *J. Catal.* **35,** 54 (1974).
85. Jung, H. J., Walker, P. L., and Vannice, M. A., *J. Catal.* **75,** 416 (1982).

86. Kellner, C. S., and Bell, A. T., *J. Catal.* **75,** 251 (1982).
87. Reuel, R. C., and Bartholomew, C. H., *J. Catal.* **85,** 78 (1984).
88. Fu, L., and Bartholomew, C. H., *J. Catal.* **92,** 376 (1985).
89. Jones, V. K., Neubauer, L. R., and Bartholomew, C. H., *J. Phys. Chem.* **90,** 4832 (1986).
90. Lin, Z., Ohukara, T., Misono, M., Tohji, K., and Udagawa, Y., *Chem. Commun.* 1673 (1986).
91. Rameswaran, M., and Bartholomew, C. H., *J. Catal.* **117,** 218 (1989).
92. Johnson, B. G., Bartholomew, C. H., and Goodman, D. W., *J. Catal.* **128,** 231 (1991).
93. Ho, S. W., Houalla, M., and Hercules, D. M., *J. Phys. Chem.* **94,** 6396 (1990).
94. Iglesia, E., Soled, S. L., and Fiato, R. A., *J. Catal.* **137,** 212 (1992).
95. Lee, J. H., Lee, D. K., and Ihm, S. K., *J. Catal.* **113,** 544 (1988).